

Investigation of Temperature Field Generated by the Tandem Submerged Arc Welding Process

Carmen-Catalina RUSU, Emil CONSTANTIN, Dan BIRSAN, Octavian MIRCEA, Daniel VISAN, Luigi-Renato MISTODIE, Bogdan GEORGESCU, Elena SCUTELNICU

Abstract— Process welding simulation is a useful tool for investigation of heat transfer, temperature field distribution, melted pool dynamics, cooling rate and, further, prediction of microstructure changes in the welded joint. The high temperature reached in the fusion zone and heat affected zone can cause phase transformations and alteration of the mechanical properties produced in the parent metal. Given the great influence of heat transfer, an accurate evaluation of temperature field generated by the welding processes is needed, in order to properly predict the base material behaviour, such as microstructure evolution, stress analysis and, finally, the quality level of the welded joint. The paper presents a detailed investigation of temperature field distribution in the case of *Tandem Submerged Arc Welding (TSAW)* process applied to join plates of pipeline steel. A 3D numerical model was developed and experimentally validated by comparing the thermal cycles achieved through finite element analysis and temperature history recorded by the temperature monitoring system developed by the authors and described in the research methodology.

Keywords—Tandem Submerged Arc Welding, FEA, infrared thermography, thermocouples

I. Introduction

Tandem welding technology is a process that involves two independent electrode wires (leading wire, LW, and trailing wire, TW) parallel arranged to the weld axis [1]. They are connected to DC and AC power sources, respectively, and individually controlled, while a distance between the leading and trailing electrode wires is constantly maintained. The advantages of the process refer to high welding speed, high productivity, defect free welds and possibility of welding plates of large thickness. Due to its advantages, such as high productivity and increased welding speed, the process is successfully applied to the pipeline manufacturing.

The pipelines used in infrastructure projects have to satisfy economical and technical conditions in order to simultaneously achieve safety in exploitation, sustainable development and environment protection.

Carmen-Catalina RUSU, Dan BIRSAN, Octavian MIRCEA, Daniel VISAN, Luigi-Renato MISTODIE, Bogdan GEORGESCU, Elena SCUTELNICU
“Dunarea de Jos” University of Galati, Faculty of Mechanical Engineering
Romania

Emil CONSTANTIN
Romanian Welding Society
Romania

The most important requirements for the pipelines, used in the oil and gas transport, are connected to the strength, plasticity and security in exploitation at extreme temperatures, different altitudes and depths. That is why, an increased attention has to be paid to the influence of thermal cycles on the mechanical and metallurgical properties of the coarse grained weld and heat affected zone (HAZ) in micro-alloyed steels.

II. FEA Modelling of Heat Transfer

Temperature field modelling is a modern method which provides the temperature field and temperature local values in the entire welded joint performed by TSAW process. Based on finite element analysis (FEA), the heat source that simulates the effect of the welding arc on the base material is considered an ellipsoid model [2]. Goldak et al. proposed a semi-ellipsoidal heat source and, further, improved into a double-ellipsoidal source in which the heat flux is distributed in a Gaussian manner throughout the volume of two semi-ellipsoids [3], [4]. The governing equation for transient heat transfer analysis is given by Eq. (1) and the spatial heat distribution, which is different in front and in the rear of the thermal source, can be computed by applying the equations (2) and (3) [3]-[5]:

$$\rho \cdot c \cdot \frac{\partial T}{\partial t}(x, y, z, t) = \nabla q(x, y, z, t) + Q(x, y, z, t) \quad (1)$$

$$q_f = \frac{6\sqrt{3}\eta \cdot Q \cdot f_f}{\pi\sqrt{\pi} \cdot a \cdot b \cdot c_f} \cdot e^{-3\left(\frac{x^2}{a^2} + \frac{y^2}{b^2} + \frac{z^2}{c_f^2}\right)} \quad (2)$$

$$q_r = \frac{6\sqrt{3}\eta \cdot Q \cdot f_r}{\pi\sqrt{\pi} \cdot a \cdot b \cdot c_r} \cdot e^{-3\left(\frac{x^2}{a^2} + \frac{y^2}{b^2} + \frac{z^2}{c_r^2}\right)} \quad (3)$$

where a, b are ellipsoidal heat source dimensions; c_f, c_r - heat source dimensions in front and rear of semi-ellipsoid; f_f, f_r - coefficients of heat apportionment in front and in the rear of semi-ellipsoid $f_f + f_r = 2$; $q(x, y, z)$ - heat flux in a certain point (x, y, z) ; Q - heat input ($Q = \eta \cdot U \cdot I$); U, I - welding voltage and amperage; η - welding process efficiency [3]-[5].

A model based on a double-ellipsoidal heat source used to simulate the *Multi-Wire Submerged Arc Welding (SAW)* process was developed in the references [6], [7]. Two ellipsoid models with different dimensions have been considered to the development of this complex numerical model. The schematic view illustrated in Figure 1 shows the position of heat sources on the pipeline steel sheets.

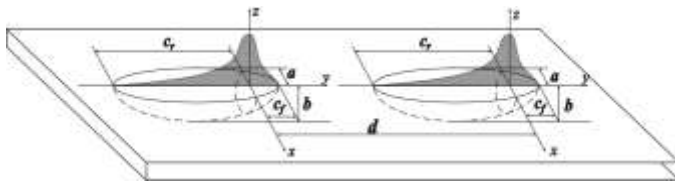


Figure 1. Sketch of heat sources positioning on sheet [5]

The thermal heat distribution, also stress and strain fields mainly depend on the welding parameters - arc voltage, welding current, welding speed - and thermo-physical and mechanical properties of the base material - the specific heat, density, conductivity, Young's modulus, Poisson's ratio - as well as the heat losses through convection and radiation processes. The following assumptions have been considered in the finite elements simulation model of TSAW:

- Thermo-physical material proprieties vs. temperature;
- Isotropy of the base material;
- Convection and radiation heat losses;
- Neglect of fluid flow in the welding pool;
- Inclusion of latent heat in the model.

The heat transfer in the welded joint of two API-5L-X70 steel plates with similar dimensions (600 × 150 × 18) mm was modelled as 3D heat transfer problem using in MSC Marc. The element type used in the analysis is SOLID 7, a three-dimensional brick element, iso-parametric with eight-nodes, which is recommended for the coupled thermal-structural analysis. In order to calculate the temperature in each element, based on the nodes temperatures, a tri-linear interpolation function was used. The temperature and heat flow gradient values are established and analyzed in all regions of the welded joint. A particular attention must be granted, in terms of refining the mesh of the model geometry, in the welded area and heat affected zone (HAZ) [5], due to the important changes that occur in this particular area, induced by the welding process. In the other parts of the model, coarser elements of the mesh were chosen, with the aim of decreasing the processing time of FEA.

The 3D model developed comprises 72,000 elements and 82,517 nodes. By the total number of 72,000 elements, 2000 elements have been assigned to the weld performed by TSAW. By applying a specific technique of finite element analysis, these elements are disabled at the beginning of the simulation and are activated when the moving heat source passes along the groove. In this way it is possible to simulate the deposition of the filler metal in the welded joint area [8].

The weld and base material, two different bodies, were considered in direct contact, in the numerical model. At the interface between the weld and base material, the value of conduction heat transfer coefficient was considered $1.0 \times 10^6 \text{ W/m}^2/\text{C}$ [8]. For the welding processes simulation, in order to minimize the errors of the numerical model, the input data (welding parameters and the dimensions of the melted pool) were collected from the experimental procedure. Based on the

data presented in Table I, the spatial heat distribution in front and behind was computed for both heat sources. In this study case, which refers to TSAW process simulation, because the heat sources act in the same welding pool, the distance between the wires was limited to 15 mm. The model took into consideration the sequence of the longitudinal welding performed on the sheet: the first welding pass (FWP) - when the pipeline steel plate is welded on the one side - and the second welding pass (SWP) - when the sheet is welded on the other side and the groove is completely filled. The welding parameters presented in table I are similar for the both passes.

TABLE I. HEAT SOURCES DIMENSIONS AND WELDING PARAMETERS

| Heat sources dimensions [mm] | | Wire | Amperage [A] | Voltage [V] | Welding speed [m/min] |
|------------------------------|----|------|--------------|-------------|-----------------------|
| a | 18 | 1 | 730 | 31 | 1,1 |
| b | 6 | | | | |
| c _f | 9 | 2 | 650 | 35 | |
| c _r | 59 | | | | |

Temperature field distribution at t=55s from the SWP of the process is presented in figure 2. It can be observed that the peak temperature is 1997°C and is reached in the centre of the second heat source. This is due the fact that the first heat source plays a role of “preheating” the cooler areas in front of the welding sources .

The numerical results obtained by FEA were processed and the thermal cycles of the nodes located at different distances (0, 4, 6, 8 and 10 mm) in cross-section from the weld axis were plotted, as figure 3 illustrates. Obviously, the peak temperature is reached on the axis of the weld, in the centre of the second heat source.

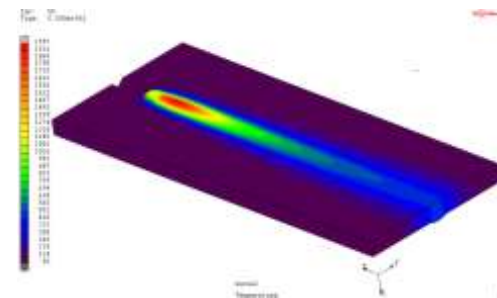


Figure 2. Temperature field distribution at t = 55s (SWP)

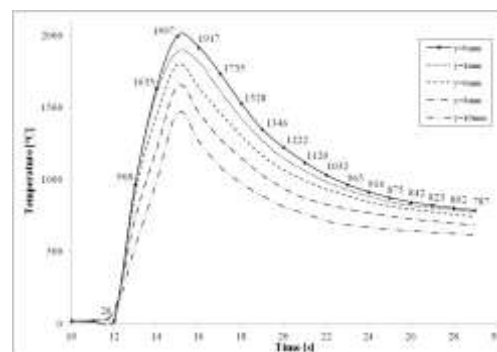


Figure 3. Thermal cycles in nodes located at different distances in cross-section of the welded joint

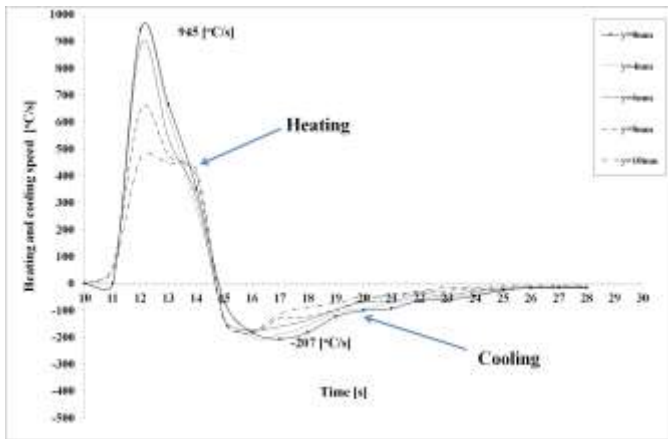


Figure 4. Heating and cooling rates recorded in TSAW process

Considering the nodes of ($x=250\text{mm}$, $y=0.4, 6, 8, 10\text{ mm}$ and $z= 9\text{mm}$) coordinates, the heating/cooling rates can be evaluated. Thus, for the above described points - located on the sheets thickness, in the melted pool, HAZ and base material - the heating and cooling speed variation is presented in figure 4. In the heating phase, the heating rate has a positive variation in time, while in the cooling phase the cooling rate has a negative variation. Also, the highest variation of the heating/cooling rate is located in the centre of the melted pool, where large temperature gradients and high temperatures are found, and continuously decreases far away from the centre of the heat source. An important issue is related to the heating and cooling rates in HAZ, area in which the mechanical and metallurgical characteristics of the material are most affected. As figure 4 reveals, the maximum heating rate is 945°C/s , while the maximum cooling rate is 207°C/s .

Analyzing the graphical processing of heating and cooling rates, presented in figure 4, and comparing with results reported in references [9] and [10], related to other welding procedures as single-wire SAW process, lower cooling speed has been identified in the TSAW process case. This feature of TSAW represents an important advantage referred to the reducing of the brittle compounds development risk. On the other hand, increased deposition rates reflected in high productivity make from TSAW process a very attractive and joining efficient technique.

III. Experimental procedure

A temperature monitoring system was designed and developed by the authors for the experimental validation of the temperature field generated by the TSAW process and assessment of heating and cooling rates. The monitoring system comprises K-type thermocouples inserted in threaded holes made in the plates. The monitoring system includes also an infrared camera positioned under the plates in order to collect data about the temperature field distribution during the entire welding process. The TC1 and TC2 thermocouples collected the temperature values recorded in the performing phase of the second filled pass, in cross section of the plates, during the TSAW process (Figure 5). The thermocouples were

inserted in threaded holes, at 9 mm distance from the bottom of sheets and 15 mm distance from the welding axis.

The TSAW process was performed in three passes: one root pass and two passes to completely fill the X gap (Figure 5). The root pass (1) was performed by *Gas Metal Arc Welding* (GMAW) process, using filled electrode wire of 1.2 mm diameter and Corgon 18 protective gas (18 l/min flow rate).

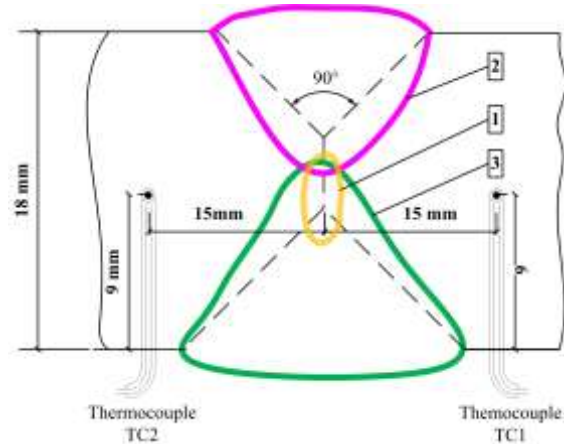


Figure 5. Sketch of TSAW passes sequence and TC1 – TC2 thermocouples arrangement

The welding conditions specific to each welding pass (power supply type, amperage – I , voltage – U , welding speed – w_s and wire feed speed w_{fi}) are presented in Table II. The positioning of the welding torches is presented in Figure 6. The diameter of both electrode wires was 4 mm.

TABLE II. WELDING PARAMETERS USED IN EXPERIMENTAL PROCEDURE

| Process | Power supply | Amperage [A] | Voltage [V] | Welding speed [m/min] | Wire feed speed [m/min] |
|---------|-----------------|--------------|-------------|-----------------------|-------------------------|
| GMAW | DC ⁺ | 336 | 38.5 | 0.98 | 13.5 |
| TSAW | DC ⁺ | 730 | 31 | 1.1 | 1.9 |
| | AC | 650 | 35 | 1.1 | 1.9 |

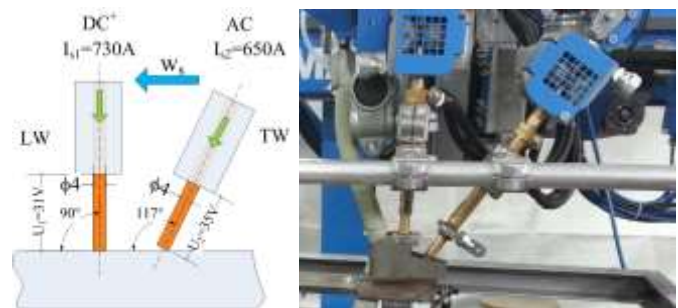


Figure 6. Positioning of welding torches (schematic and real view)

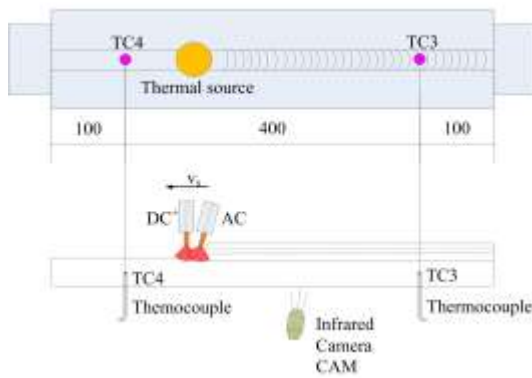


Figure 7. TC3 and TC4 thermocouples arrangement

After the root pass (FPW) was achieved, the plates were positioned upside-down and the first SWP was carried out. The TC3 and TC4 thermocouples collected the temperature values during the filling the groove by TSAW process, as figure 7 presents. The thermocouples were positioned in threaded holes performed in the weld at 100 mm distance from the lateral edges of the sheets and 10 mm distance from bottom of (FWP) weld. Moreover, an infrared camera was included in the temperature monitoring system in order to get the image of temperature field during the entire welding process.

IV. Results and discussions

In order to validate the 3D numerical model developed by the authors, a comparative analysis between the thermal cycles achieved by finite element analysis and thermal history recorded by the thermocouples and infrared camera was made in detail during the TSAW process of pipeline steel plates. The numerical and experimental results have been processed and three charts have been plotted and comparatively presented in Figure 8. The temperature values, registered during the experimental procedure with TC3 and TC4 thermocouples, encountered an offset due to their positioning at different distances in the longitudinal plane of the welded joint (the distance between thermocouples was fixed at 400 mm). The TC3 and TC4 thermocouples were positioned in the weld after performing FWP and registered higher values of temperature compared with the ones recorded by thermocouples TC1 and TC2, during the FWP. The thermal cycle (FEM), based on FEA outcomes, was plotted in the location of TC4 thermocouple. The peak temperature reached 600°C. A good match between numerical and experimental results has been identified. Also a reduced cooling rate, having, positive effects on the plasticity of the weld, was noticed in case of TSAW process.

The experimental program focused on the temperature field analysis using thermography method. Infrared thermography, a non-contact temperature measurement method, is the technique of creating fully analyzable images, from the thermal radiation given by an object, using an infrared camera [11].

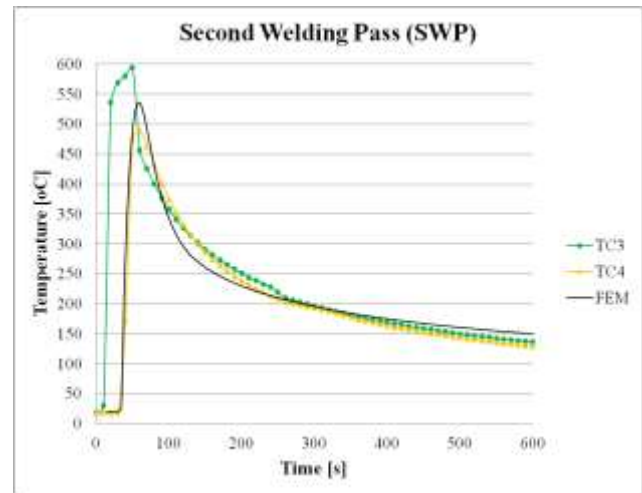


Figure 8. Temperature vs. time in TSAW process

The infrared camera used in experiments was Flir A20M and was positioned under the sheets due to the fact that the welding flux used for arc protection covers the welded joint surface and the interest area cannot be monitored. Figure 9 presents a thermal image achieved during the performing of SWP by TSAW process. In order to study the temperature variation on the longitudinal axis, a LI01 line marker was traced on the thermal image (thermogram). The software incorporated in the thermography monitoring system allows the processing of experimental results and provides the infrared image of the temperature field distribution, at a certain moment of the process, and the thermal cycle required for any spot of the welded joint.

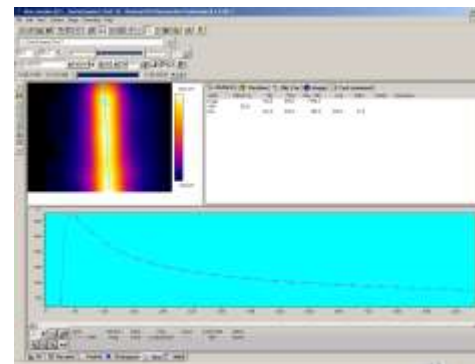


Figure 9. Temperature field capture and thermal history achieved through the infrared camera

V. Conclusions

Based on the investigations focussed on the monitoring of temperature field, the following conclusions emerged:

- taking into account the Goldak equations specific to the elliptical thermal sources, a 3D numerical model useful for the simulation of TSAW process was developed by the authors;

- variation of temperature in the welded joint areas was numerically and experimentally determined and deeply analyzed; as the weld and HAZ areas are the most affected by the welding process and could be considered the most interesting regions in the analysis of the base material behaviour, a mesh refining was designed and developed in these strips;
- applying the movement technique, finite elements associated to the welding filler material were disabled at the beginning of the simulation and activated when the moving heat sources passed along the groove;
- the real welding time of the TSAW process is identical with the total finite element analysis time;
- thermal cycles were plotted in points/nodes positioned in the longitudinal/cross-section plane of the welded joint axis;
- charts were drawn for the analysis of heating and cooling rates; due to the additional heat generated by the second welding source, the cooling rates are lower in the case of TSAW process in comparison with single-wire SAW process. This phenomenon is beneficial and reduces the risk of brittle compounds occurrence in the weld and HAZ regions;
- the validation of the 3D mathematical model was performed, by comparing the thermal cycles obtained through finite element analysis and those measured by the temperature monitoring system designed and developed by the authors.

In conclusion, the three-dimensional mathematical model developed for the simulation of TSAW process can be applied with accuracy for prediction of the temperature fields, thermal cycles and heating/cooling rates generated and induced, respectively, by the welding process.

Acknowledgment

This work was supported by a grant of the Romanian National Authority for Scientific Research, CNDI–UEFISCDI, project number PN-II-PT-PCCA-2011-3.1-1057.

References

- [1] D.V. Kiran, D.W. Cho, W.H. Song, S.J. Na, "Arc behavior in two wire tandem submerged arc welding", *Journal of Materials Processing Technology*, Volume 214, Issue 8, August 2014, pp. 1546-1556
- [2] J. Y. Lee, J. M. Park, C. H. Lee, E. P. Yoon, "Synthesis/Processing of Lightweight Metallic Materials II", Eds. C. M. Ward-Close, F. H. Froes, S. S. Cho and D. J. Chellman, The Minerals, Metals and Materials Society, Warrendale, PA, 1996, p. 49. apud Sindo, Kou, *Welding Metallurgy*, John Wiley & Sons, Inc., Hoboken, New Jersey, USA, 2003, p. 55
- [3] J. Goldak, M. Bibby, J. Moore, R. House, B. Patel, "Computer modeling of heat flow in welds", *Metallurgical Transactions B*, vol. 17 B, 1986, pp. 587-600.
- [4] F. Kong, J. Ma, R. Kovacevic, "Numerical and experimental study of thermally induced residual stress in the hybrid laser–GMA welding

- process", *Journal of Materials Processing Technology* 211 (2011) 1102–1111 apud J. Goldak, A. Chakravarti, M. Bibby, "A new finite element model for welding heat source", *Metallurgical Transactions B* 15B, 1984, 299–305
- [5] E. Scutelnicu, C. C. Rusu, "Assessment of Cooling Rate in Longitudinal Welded Pipelines performed by Submerged Double-Arc Welding", *International Journal of Mechanics*, Volume 8, 2014, ISSN1998-4448, pp. 144-149
- [6] D.W. Choa, D. V. Kiranb, W.H Songc, S.J Na, "Molten pool behavior in the tandem submerged arc welding process", *Journal of Materials Processing Technology*, Volume 214, Issue 11, November 2014, pp. 2233–2247
- [7] S. Moeinifara, A.H. Kokabib, H.R. Madaah Hosseinib, "Role of tandem submerged arc welding thermal cycles on properties of the heat affected zone in X80 microalloyed pipe line steel", *Journal of Materials Processing Technology*, Volume 211, Issue 3, 1 March 2011, pp. 368–375
- [8] D.C. Birsan, E. Scutelnicu, D. Visan, "Modeling of Heat Transfer in Pipeline Steel Joint Performed by Submerged Double-Arc Welding Procedure", *Advanced Materials Research*, Vol. 814, 2013, pp. 33-40, doi: 10.4028/www.scientific.net/AMR.814.33
- [9] Rusu C.C., Scutelnicu E., Mistodie L.R., Temperature field analysis of API 5L-X70 steel joint performed by submerged double arc welding, *Proceedings of the European Federation for Welding - EWF Eurojoin 8 Conference*, 24-26 May 2012, Pola-Croatia, ISBN 978-953-7518-02-8, pag. 231-240
- [10] Mistodie L.R., Rusu C.C., Constantin E., Scutelnicu E., Voicu C., Comparative experimental study on mono and multiarc submerged arc welding of API 5L-X70 steel, *Proceedings of the European Federation for Welding - EWF Eurojoin 8 Conference*, 24-26 May 2012, Pola-Croatia, ISBN978-953-7518-02-8, pag. 125-132
- [11] L.R. Mistodie, C. Toma, C. C. Rusu, "Determinarea experimentală a campului termic la sudarea multiarc sub strat de flux a tevilor utilizate la fabricarea conductelor magistrale", *Proceedings of ASR Conference Sudura, Sibiu*, 2014